arXiv:1610.03351v3 [astro-ph.CO] 13 Dec 2016

A general relativistic signature in the galaxy bispectrum

Obinna Umeh[1], Sheean Jolicoeur[1], Roy Maartens[1,2], Chris Clarkson[3,4]

[1] *Department of Physics & Astronomy, University of the Western Cape, Cape Town 7535, South Africa*
[2] *Institute of Cosmology & Gravitation, University of Portsmouth, Portsmouth PO1 3FX, UK*
[3] *School of Physics & Astronomy, Queen Mary University of London, London E1 4NS, UK*
[4] *Department of Mathematics & Applied Mathematics, University of Cape Town, Cape Town 7701, South Africa*

(Dated: December 14, 2016)

Next-generation galaxy surveys will increasingly rely on the galaxy bispectrum to improve cosmological constraints, especially on primordial non-Gaussianity. A key theoretical requirement that remains to be developed is the analysis of general relativistic effects on the bispectrum, which arise from observing galaxies on the past lightcone. Here we compute for the first time all the local relativistic corrections to the bispectrum, from Doppler, gravitational potential and higher-order effects. For the galaxy bispectrum, the problem is much more complex than for the power spectrum, since we need the lightcone corrections at second order. Mode-coupling contributions at second order mean that relativistic corrections can be non-negligible at smaller scales than in the case of the power spectrum. In a primordial Gaussian universe, we show that the relativistic bispectrum for a moderately squeezed shape can differ from the Newtonian prediction by $\sim 3\%$ when the short modes are at the equality scale. For the equilateral shape, the difference is $\sim 60\%$ at gigaparsec scales. The relativistic corrections, if ignored in the analysis of observations, could therefore easily be mistaken for primordial non-Gaussianity. We conclude that for upcoming surveys which probe equality scales and beyond, these new relativistic signatures must be included for an accurate measurement of primordial non-Gaussianity.

Introduction

With the coming generation of large-scale surveys, the galaxy bispectrum will play an increasingly important role, supplementing the power spectrum. In particular, the bispectrum will be crucial in discriminating inflationary models via constraints on primordial non-Gaussianity [1].

It is well known that the primordial signal is contaminated by nonlinearity in the matter overdensity and in the galaxy bias, which requires accurate modelling for cosmological constraints and forecasts. Here we focus on a lesser known source of non-Gaussianity, i.e. the 'projection' effects that arise from observing on the past lightcone. These general relativistic effects are inescapably present in the measurements and lead to a contamination of the primordial signal. The standard Newtonian analysis of the bispectrum incorporates the projection effect due to redshift-space distortions, but omits the other projection effects. At the relatively low redshifts and small sky areas probed by current surveys, this approximation is reasonable. However, for next-generation surveys, the Newtonian approximation cannot be expected to deliver the necessary theoretical accuracy.

Recently, [2] computed the effects of lensing on the angular bispectrum, showing that this relativistic correction to the Newtonian analysis is relevant at higher redshifts and on intermediate scales. In principle the lensing effect can be removed if we can estimate the matter density along each line of sight – i.e., surveys can in principle be de-lensed. There are further integrated relativistic corrections, from integrated Sachs-Wolfe and time delay effects and their couplings, which are expected to be much smaller. An effective way to suppress the lensing and other integrated effects is to consider only correlations at the same fixed redshift, as we do here.

We fill a key theoretical gap by computing all the local relativistic corrections from Doppler and gravitational potential effects and their nonlinear couplings. The details of the derivation are given in an accompanying paper [3]. We provide a complete result, using the full expression up to second order for relativistic effects on the observed galaxy number counts [4] (see also [5–8]). Our result is valid for arbitrary triangle shapes in Fourier space. This generalizes the partial result of [9], which applied a separate universe analysis to estimate the relativistic effects in the special case of a squeezed bispectrum.

Bispectrum in general relativity

The observed galaxy number density contrast at redshift z and in direction $\boldsymbol{n}$ is denoted by $\Delta_g(z,\boldsymbol{n})$. Since it is observable, Δ_g is a gauge-independent quantity, and any gauge can be used to compute it. We only consider correlations at the same redshift. At fixed redshift z, the galaxy 3-point correlation function depends on $\boldsymbol{n}_i$ ($i=1,2,3$) and can be computed as the bispectrum in Fourier space at fixed $\eta(z)$, with $\boldsymbol{x}_i=(\eta_0-\eta(z))\boldsymbol{n}_i\to\boldsymbol{k}_i$. The galaxy bispectrum B_g is defined by (suppressing the redshift dependence)

$$\langle\Delta_g(\boldsymbol{k}_1)\Delta_g(\boldsymbol{k}_2)\Delta_g(\boldsymbol{k}_3)\rangle=(2\pi)^3B_g(\boldsymbol{k}_1,\boldsymbol{k}_2,\boldsymbol{k}_3)\delta^D(\boldsymbol{k}_1+\boldsymbol{k}_2+\boldsymbol{k}_3). \tag{1}$$

Integrated effects become significant when we correlate across different redshift bins, and the galaxy 3-point function cannot be converted uniquely to the bispectrum in Fourier space, requiring us to use the angular bispectrum.

We assume Gaussian initial conditions and use a local univariate model of galaxy bias [10]:

$$\delta_g(\boldsymbol{x})=b_1\delta_m(\boldsymbol{x})+\frac{1}{2}b_2\big[\delta_m(\boldsymbol{x})^2-\big\langle\delta_m(\boldsymbol{x})^2\big\rangle\big]. \tag{2}$$

We use Poisson gauge, but δ_g,δ_m are the comoving-synchronous number and density contrasts, in order to define bias correctly [4, 11]. We require $\Delta_g=\Delta_g^{(1)}+\Delta_g^{(2)}/2$ at second order if we compute B_g to leading order:

$$2\langle\Delta_g(\boldsymbol{k}_1)\Delta_g(\boldsymbol{k}_2)\Delta_g(\boldsymbol{k}_3)\rangle=\langle\Delta_g^{(1)}(\boldsymbol{k}_1)\Delta_g^{(1)}(\boldsymbol{k}_2)\Delta_g^{(2)}(\boldsymbol{k}_3)\rangle+2\text{ cyclic permutations}. \tag{3}$$

The expression that we use for $\Delta_g(z,\boldsymbol{n})$, including all general relativistic (GR) effects up to second order, is given in [4]. We neglect the integrated terms, and also the effects on Δ_g of source evolution bias and magnification bias.

At first order

$$\Delta_g^{(1)}(\boldsymbol{k})=\mathcal{K}^{(1)}(k,\mu)\delta_m^{(1)}(\boldsymbol{k}), \tag{4}$$

where the observed direction $\boldsymbol{n}$ appears through $\mu=\hat{\boldsymbol{k}}\cdot\boldsymbol{n}$. The kernel $\mathcal{K}^{(1)}(k,\mu)$ maps the dark matter density contrast to the observed galaxy number density contrast. In anticipation of the more complicated second-order kernel, we can split this into a dynamical part – from the evolution of the density contrast, and a projected part – from observational lightcone effects, each of which is the sum of a Newtonian part $\mathcal{K}_{\rm N}^{(1)}$ and a GR correction $\mathcal{K}_{\rm GR}^{(1)}$. In the Newtonian part we include the redshift-space distortions:

$$\mathcal{K}_{\rm N}^{(1)}(k,\mu)=b_1+f\mu^2\,, \tag{5}$$

where $f=-\mathrm{d}\ln D/\mathrm{d}\ln(1+z)$ is the linear growth rate. The GR correction is [11, 12]

$$\mathcal{K}_{\rm GR}^{(1)}(k,\mu)\;=\;-\mathrm{i}f\left[\frac{2}{\chi\mathcal{H}}+\frac{\mathcal{H}'}{\mathcal{H}^2}\right]\mu\frac{\mathcal{H}}{k}+\left[3f+\frac{3}{2}\Omega_m\left(2-f-\frac{2}{\chi\mathcal{H}}-\frac{\mathcal{H}'}{\mathcal{H}^2}\right)\right]\frac{\mathcal{H}^2}{k^2}\equiv\mathrm{i}\gamma_1\frac{\mu}{k}+\frac{\gamma_2}{k^2}, \tag{6}$$

where $\chi=\eta_0-\eta$. The $\mathcal{H}/k$ term arises from Doppler effects, and the $(\mathcal{H}/k)^2$ term is due to gravitational potentials (we have used the GR Poisson and Euler equations).

At second order

$$\Delta_g^{(2)}(\boldsymbol{k})=\int\frac{\mathrm{d}^3k_1}{(2\pi)^3}\int\mathrm{d}^3k_2\,\mathcal{K}^{(2)}(\boldsymbol{k}_1,\boldsymbol{k}_2,\boldsymbol{k})\delta_m^{(1)}(\boldsymbol{k}_1)\delta_m^{(1)}(\boldsymbol{k}_2)\delta^D(\boldsymbol{k}_1+\boldsymbol{k}_2-\boldsymbol{k}). \tag{7}$$

We again split the kernel into Newtonian and GR correction terms, each of which consists of evolution terms and projection effects. We neglect the GR corrections to the evolution of the density contrast since our focus is on projection effects (see [13–15] for the GR dynamical corrections). The Newtonian part is

$$\mathcal{K}_{\rm N}^{(2)}(\boldsymbol{k}_1,\boldsymbol{k}_2,\boldsymbol{k}_3)=b_1F_2(\boldsymbol{k}_1,\boldsymbol{k}_2)+b_2+f\,G_2(\boldsymbol{k}_1,\boldsymbol{k}_2)\mu_3^2+\mathcal{Z}_2(\boldsymbol{k}_1,\boldsymbol{k}_2), \tag{8}$$

where $\mu_i=\hat{\boldsymbol{k}}_i\cdot\boldsymbol{n}$. The first 3 terms on the right are dynamical and the last term is projection. The kernels in (8) are given by [16, 17]

$$F_2(\boldsymbol{k}_1,\boldsymbol{k}_2)\;=\;\frac{10}{7}+\frac{\boldsymbol{k}_1\cdot\boldsymbol{k}_2}{k_1k_2}\left(\frac{k_1}{k_2}+\frac{k_2}{k_1}\right)+\frac{4}{7}\left(\frac{\boldsymbol{k}_1\cdot\boldsymbol{k}_2}{k_1k_2}\right)^2, \tag{9}$$

$$G_2(\boldsymbol{k}_1,\boldsymbol{k}_2)\;=\;\frac{6}{7}+\frac{\boldsymbol{k}_1\cdot\boldsymbol{k}_2}{k_1k_2}\left(\frac{k_1}{k_2}+\frac{k_2}{k_1}\right)+\frac{8}{7}\left(\frac{\boldsymbol{k}_1\cdot\boldsymbol{k}_2}{k_1k_2}\right)^2, \tag{10}$$

$$\mathcal{Z}_2(\boldsymbol{k}_1,\boldsymbol{k}_2)\;=\;f^2\frac{\mu_1\mu_2}{k_1k_2}\big(\mu_1k_1+\mu_2k_2\big)^2+b_1\frac{f}{k_1k_2}\left[\big(\mu_1^2+\mu_2^2\big)k_1k_2+\mu_1\mu_2\big(k_1^2+k_2^2\big)\right]. \tag{11}$$

These kernels describe respectively the nonlinear effects from the density contrast, peculiar velocities and redshift-space distortions. Note that the overall scaling with k for $\mathcal{K}_{\rm N}^{(2)}$ is $\mathcal{O}(k^0)$: only the angles between the observed direction $\boldsymbol{n}$ and $\boldsymbol{k}_i$ appear.

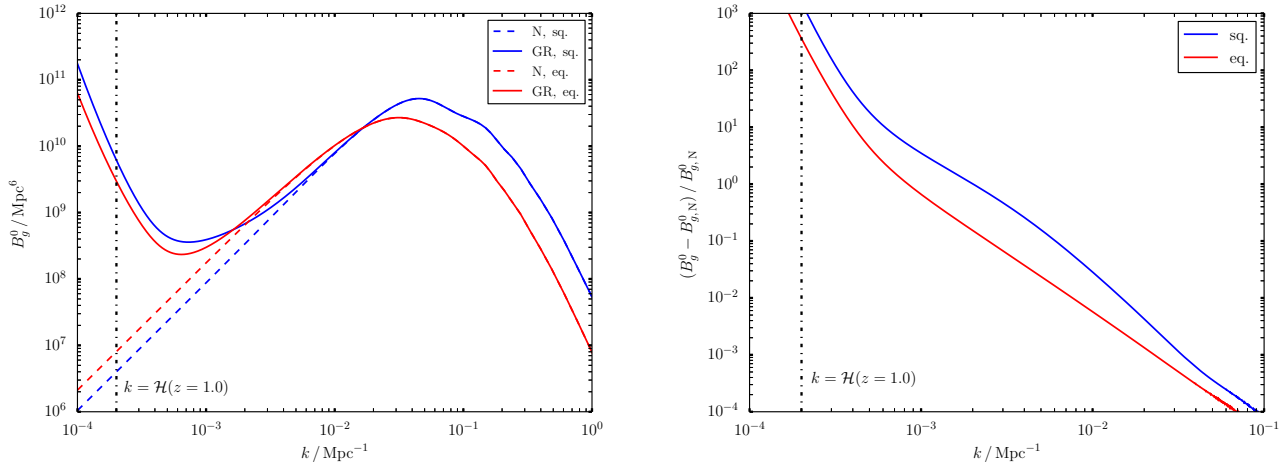

FIG. 1: *Left:* Monopole of the bispectrum including all GR corrections (GR, solid) compared to its Newtonian approximation (N, dashed), for equilateral (eq., red) and squeezed (sq., blue) triangles. *Right:* Fractional difference due to GR corrections. (Note: the Hubble constant is fixed at $h = 0.678$.)

The computation of the GR correction kernel is a key result of this work (see [3] for details):[1]

$$\begin{aligned}\mathcal{K}_{\rm GR}^{(2)}(\boldsymbol{k}_1,\boldsymbol{k}_2,\boldsymbol{k}_3) = \frac{1}{k_1^2k_2^2}\Bigg\{&\Gamma_1 + \mathrm{i}\,(\mu_1k_1+\mu_2k_2)\,\Gamma_2 + \left(\frac{k_1k_2}{k_3}\right)^2\Big[F_2(\boldsymbol{k}_1,\boldsymbol{k}_2)\Gamma_3 + G_2(\boldsymbol{k}_1,\boldsymbol{k}_2)\Gamma_4\Big]\\ &+ \mu_1\mu_2k_1k_2\,\Gamma_5 + (\boldsymbol{k}_1\cdot\boldsymbol{k}_2)\,\Gamma_6 + \left(k_1^2+k_2^2\right)\Gamma_7 + (\mu_1^2k_1^2+\mu_2^2k_2^2)\Gamma_8\\ &+ \mathrm{i}\Bigg[\left(\mu_1k_1^3+\mu_2k_2^3\right)\Gamma_9 + (\mu_1k_1+\mu_2k_2)\,(\boldsymbol{k}_1\cdot\boldsymbol{k}_2)\,\Gamma_{10} + k_1k_2\,(\mu_1k_2+\mu_2k_1)\,\Gamma_{11}\\ &+ (\mu_1^3k_1^3+\mu_2^3k_2^3)\,\Gamma_{12} + \mu_1\mu_2k_1k_2\,(\mu_1k_1+\mu_2k_2)\,\Gamma_{13} + \mu_3\frac{k_1^2k_2^2}{k_3}G_2(\boldsymbol{k}_1,\boldsymbol{k}_2)\Gamma_{14}\Bigg]\Bigg\},\end{aligned} \tag{12}$$

where $\Gamma_I(z)$ are given in the Appendix. In contrast to the Newtonian kernel, the GR correction terms have scalings from $\mathcal{O}(k^{-4})$ to $\mathcal{O}(k^{-1})$, so that they are suppressed on small scales. The leading order GR corrections (6) to the power spectrum are linear and are confined to ultra-large scales. By contrast, the leading order GR corrections to the bispectrum are nonlinear – and mode coupling between linear GR corrections and Newtonian terms means that the GR corrections in the bispectrum are present on smaller scales than in the power spectrum.

Using Wick's theorem,

$$B_g(\boldsymbol{k}_1,\boldsymbol{k}_2,\boldsymbol{k}_3) = \mathcal{K}^{(1)}(\boldsymbol{k}_1)\mathcal{K}^{(1)}(\boldsymbol{k}_2)\mathcal{K}^{(2)}(\boldsymbol{k}_1,\boldsymbol{k}_2,\boldsymbol{k}_3)P(k_1)P(k_2) + 2\text{ cyclic permutations}\,, \tag{13}$$

where $P(k)$ is the linear matter power spectrum. In the squeezed limit, $k_2 \approx k_3 = k_S \gg k_L = k_3$, we can give an

[1] Γ_2 in arXiv v2 has been absorbed into Γ_1; the previous $\Gamma_I, I = 3,\cdots,14$ have been re-labelled $I = 2,\cdots,13$, and the new Γ_{14} term here is a correction to arXiv v2.

analytical formula for the monopole $B_g^{\mathrm{sq}\,0} = (1/2)\int_{-1}^{+1} \mathrm{d}\mu_1 B_g^{\mathrm{sq}}$ (see [18] for details):

$$B_g^{\mathrm{sq}\,0}(k_L, k_S) = \left\{ \left[\frac{2}{105}\Big(80b_1 f + 21 b_1 f^2 + 150 b_1^2 + 35 b_1^2 f + 105 b_1 b_2 + 35 b_2 f + 18 f^2\Big)\gamma_2 + \frac{2}{3} b_1 \big(3b_1 + f\big)\Gamma_7 + \frac{2}{15} b_1 \big(5b_1 + 3f\big)\Gamma_8 \right] \frac{1}{k_L^2} + \left[\frac{2}{15}\gamma_2 \Big(5\big(3b_1 + f\big)\Gamma_7 + \big(5b_1 + 3f\big)\Gamma_8\Big)\right] \frac{1}{k_L^4} \right\} P(k_L) P(k_S), \tag{14}$$

where γ_2 is defined by (6).

In order to illustrate the nature and magnitude of the GR corrections to the bispectrum, we choose an isosceles configuration, with $k_1 = k_2 \equiv k$ and $k_3 = k\sqrt{2(1-\cos\theta_{12})}$. We consider the cases of equilateral ($\theta_{12} = \pi/3$) and squeezed ($\theta_{12} \ll 1$) triangles, and we set the redshift to $z = 1$. For the galaxy bias, we take $b_1 = \sqrt{1+z}$ and $b_2 = -0.3\sqrt{1+z}$. The cosmological parameters are those from Planck 2015 [19]. In Fig. 1, the monopole of the full bispectrum with GR corrections is compared to the Newtonian approximation.

Squeezed shapes: We choose $\cos\theta_{12} = 0.998$ so that $k_3 \approx k/16$. Even for this moderately squeezed case we see a significant departure from the Newtonian prediction when the short-wavelength sides k (long sides in Fourier space) approach the equality scale: the difference is $\gtrsim 3\%$ for $k \lesssim 10^{-2}\,\mathrm{Mpc}^{-1}$. Because of mode coupling, the GR correction reaches percent-level at surprisingly small scales, just below the equality scale. If we take the current Hubble scale as an observable upper limit for the triangle sides, the long-wavelength side is a maximum when $k_3 = H_0 \approx 2.3\times10^{-4}\,\mathrm{Mpc}^{-1}$, corresponding to $k \approx 16 k_3 \approx (270\,\mathrm{Mpc})^{-1}$. At this maximum, the GR bispectrum is ~ 1.3 times the Newtonian prediction.

Equilateral shapes: We see a similar behaviour, with a difference of $\sim 0.6\%$ at equality scales and $\gtrsim 60\%$ when $k = k_3 \lesssim 1\,\mathrm{Gpc}^{-1}$. The GR correction reaches percent-level at $k \sim (130\,\mathrm{Mpc})^{-1}$. The equal wavelengths of the triangle are at the observable maximum when $k = k_3 = H_0$. At this maximum, the GR bispectrum is ~ 350 times the Newtonian prediction.

We define the reduced monopole of the bispectrum (including GR corrections) as

$$Q(\boldsymbol{k}_1, \boldsymbol{k}_2, \boldsymbol{k}_3) = \frac{B_g^0(\boldsymbol{k}_1, \boldsymbol{k}_2, \boldsymbol{k}_3)}{\big[P_g^0(\boldsymbol{k}_1)P_g^0(\boldsymbol{k}_2) + 2 \text{ cyclic permutations}\big]}\,, \tag{15}$$

where P_g^0 is the monopole of the linear galaxy power spectrum including GR corrections at first order. In the Newtonian approximation, B_g^0 in (15) is replaced by $B_{g,\mathrm{N}}^0$ and P_g^0 is replaced by the monopole of the Newtonian galaxy power spectrum (including redshift-space distortions).

The dimensionless reduced monopole of the bispectrum, as a function of the angle θ_{12}, is shown in Fig. 2, for scales $k \approx k_{\mathrm{eq}}$ and $k = 1\,\mathrm{Gpc}^{-1}$. In the equality-scale case, the fractional GR correction is percent-level except for $0.3 \lesssim \theta_{12}/\pi \lesssim 0.8$, where it is sub-percent. For the gigaparsec scale, the fractional GR correction is $\gtrsim 30\%$ for all θ_{12}, reaching $\sim 200\%$ for $\theta_{12}/\pi = 0$ or 1.

Misinterpreting the primordial universe

We see from Figs. 1 and 2 how GR projection effects, in a Gaussian primordial universe, boost the large and ultra-large scale power in the bispectrum. This behaviour is qualitatively similar to the effect of primordial non-Gaussianity on the Newtonian bispectrum. In a Newtonian analysis, one needs to subtract off the nonlinear effects from evolution and from redshift-space distortions in order to isolate the primordial non-Gaussian signal. Our results show that GR projection effects contribute a significant contamination – a Newtonian analysis of the bispectrum, in the case where equality scales and larger are being probed, could be seriously misleading by ignoring the GR projection effects.

For a simple illustration, we consider the effect of local primordial non-Gaussianity on the Newtonian galaxy bispectrum, but we neglect the scale-dependence in the galaxy bias. The primordial gravitational potential is

$$\Phi^{\mathrm{nG}}(\boldsymbol{x}) = \varphi(\boldsymbol{x}) + f_{\mathrm{NL}}\left(\varphi(\boldsymbol{x})^2 - \big\langle\varphi(\boldsymbol{x})^2\big\rangle\right), \tag{16}$$

where φ is a first-order Gaussian potential. As a consequence, the matter density contrast receives a correction:

$$\delta_m^{\mathrm{nG}}(z, \boldsymbol{k}) = \alpha(z,k)\left[\varphi(\boldsymbol{k}) + f_{\mathrm{NL}}\int \frac{\mathrm{d}^3k'}{(2\pi)^3}\varphi(\boldsymbol{k}')\varphi(\boldsymbol{k}-\boldsymbol{k}')\right] \quad \text{with} \quad \alpha(k,z) = \frac{2k^2 D(z)T(k)}{3H_0^2\Omega_{m0}}\frac{g(z=0)}{g(z_\infty)}, \tag{17}$$

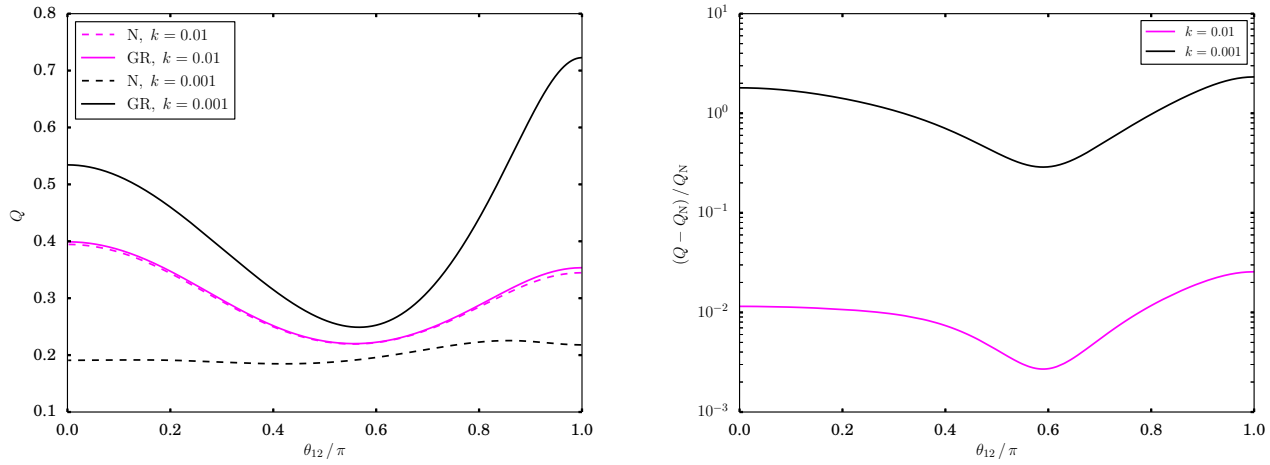

FIG. 2: *Left:* General relativistic reduced monopole of the bispectrum (GR, solid) compared to the Newtonian approximation (N, dashed), as a function of the isosceles angle, for equality-scale (magenta) and Gpc-scale (black) wavelengths of the equal sides k. *Right:* Fractional correction from GR effects.

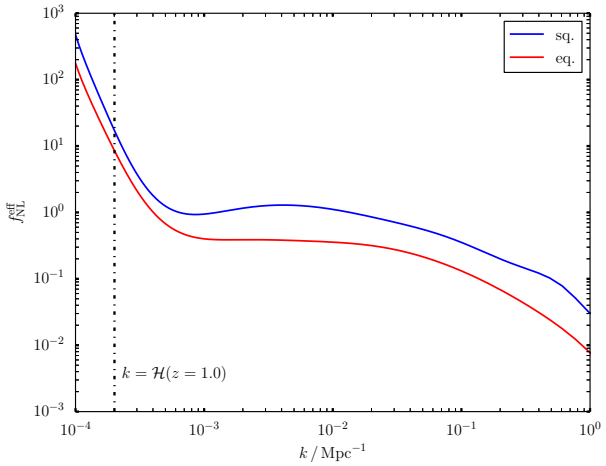

FIG. 3: Effective non-Gaussianity due to GR corrections from comparing to a Newtonian analysis, neglecting scale-dependent galaxy bias. (Curves correspond to the cases considered in Fig. 1.)

where T is the transfer function ($T \to 1$ for $k \to 0$), and $g = (1+z)D$ is the growth suppression factor. Then a Newtonian analysis of the bispectrum, neglecting scale-dependence in the galaxy bias, leads to

$$B^{\rm nG}_{g,{\rm N}}(\boldsymbol{k}_1,\boldsymbol{k}_2,\boldsymbol{k}_3) \;=\; \mathcal{K}^{(1)}_{\rm N}(\boldsymbol{k}_1)\mathcal{K}^{(1)}_{\rm N}(\boldsymbol{k}_2)\left[\mathcal{K}^{(2)}_{\rm N}(\boldsymbol{k}_1,\boldsymbol{k}_2,\boldsymbol{k}_3)+2f_{\rm NL}\mathcal{K}^{(1)}_{\rm N}(\boldsymbol{k}_3)\frac{\alpha(k_3)}{\alpha(k_1)\alpha(k_2)}\right]P(k_1)P(k_2)$$
$$+\,2\ \text{cyclic permutations}\,. \qquad (18)$$

Suppose that we interpret the observed galaxy bispectrum using the standard Newtonian analysis. In order to fit the observations we would match the theoretical bispectrum (18) to the observed bispectrum. However, the observed bispectrum necessarily includes the GR corrections from projection effects. Therefore, we would effectively

be matching (18) to (13). This would produce an effective $f_{\rm NL}^{\rm eff}$:

$$f_{\rm NL}^{\rm eff}(\boldsymbol{k}_1,\boldsymbol{k}_2,\boldsymbol{k}_3) = \left\{ \left[\mathcal{K}_{\rm GR}^{(1)}(\boldsymbol{k}_1)\mathcal{K}^{(1)}(\boldsymbol{k}_2)\mathcal{K}^{(2)}(\boldsymbol{k}_1,\boldsymbol{k}_2,\boldsymbol{k}_3) + \mathcal{K}_{\rm N}^{(1)}(\boldsymbol{k}_1)\mathcal{K}_{\rm GR}^{(1)}(\boldsymbol{k}_2)\mathcal{K}^{(2)}(\boldsymbol{k}_1,\boldsymbol{k}_2,\boldsymbol{k}_3) + \mathcal{K}_{\rm N}^{(1)}(\boldsymbol{k}_1)\mathcal{K}_{\rm N}^{(1)}(\boldsymbol{k}_2)\mathcal{K}_{\rm GR}^{(2)}(\boldsymbol{k}_1,\boldsymbol{k}_2,\boldsymbol{k}_3)\right] P(k_1)P(k_2) + 2 \text{ cyclic permutations} \right\} \times \left\{ 2\mathcal{K}_{\rm N}^{(1)}(\boldsymbol{k}_1)\mathcal{K}_{\rm N}^{(1)}(\boldsymbol{k}_2)\mathcal{K}_{\rm N}^{(1)}(\boldsymbol{k}_3)\frac{\alpha(k_3)}{\alpha(k_1)\alpha(k_2)}P(k_1)P(k_2) + 2 \text{ cyclic permutations} \right\}^{-1}. \quad (19)$$

Figure 3 shows $f_{\rm NL}^{\rm eff}$. At equality scales, $f_{\rm NL}^{\rm eff} \sim 0.3$ for the equilateral and ~ 1 for the squeezed case. On the false basis of a Newtonian interpretation, we would conclude that the primordial universe was significantly non-Gaussian and that the non-Gaussianity was of nonlocal type. Of course, we have neglected the scale-dependent galaxy bias that is induced by local primordial non-Gaussianity. This scale-dependent bias produces similar effects to the GR light-cone effects – which reinforces our conclusion that the GR lightcone effects need to be included for a consistent analysis.

Conclusions

Non-Gaussianity in the galaxy distribution arises from three effects – primordial, evolution and projection effects. The standard Newtonian analysis includes only the projection effects from redshift-space distortions. This has been extended by [2] to include the GR projection effect of weak lensing. We have computed for the first time the galaxy bispectrum in a primordial Gaussian universe, with all local GR projection effects included, up to second order. Our key results are the nonlinear GR correction kernel (12) and the analytical form of the squeezed limit of the galaxy bispectrum (14). GR effects in the galaxy bispectrum for isosceles shapes are shown in Figs. 1 and 2.

A major aim of future galaxy surveys is to measure primordial non-Gaussianity with precision down to $|f_{\rm NL}| < 1$, beyond the capabilities of CMB experiments, using both the power spectrum [20, 21] and bispectrum [1]. It is known that neglecting GR projection effects in the galaxy power spectrum can bias the measurement of $f_{\rm NL}$ [22, 23]. We have extended this to the galaxy bispectrum, showing how nonlinear GR projection effects will contaminate the primordial non-Gaussian signal. The mode coupling present at leading order in the bispectrum means that the GR effects can be non-negligible at smaller scales than for the power spectrum.

The strongest effects arise for squeezed shapes: with moderate squeezing, the GR correction to the bispectrum is $\sim 3\%$ of the Newtonian prediction when the short-wavelength sides are at equality scales. At the maximum observable scales, the GR bispectrum is ~ 1.3 times the Newtonian prediction. For equilateral shapes, the GR correction to the bispectrum reaches percent-level at $k \sim (130\,{\rm Mpc})^{-1}$, and is $\sim 60\%$ of the Newtonian bispectrum at gigaparsec scales.

It is therefore essential for an accurate measurement of $f_{\rm NL}$ to incorporate the GR lightcone effects in theoretical analysis of the galaxy bispectrum for next-generation surveys. Our results motivate systematic further work to forecast the signal to noise of the GR corrections for various next-generation surveys.

Acknowledgments:
We thank Daniele Bertacca, Ruth Durrer, Kazuya Koyama, Sabino Matarrese and David Wands for useful discussions and comments. All authors are funded in part by the NRF (South Africa). OU, SJ and RM are also supported by the South African SKA Project. RM is also supported by the UK STFC, Grants ST/K00090X/1 and ST/N000668/1.

[1] M. Tellarini, A. J. Ross, G. Tasinato and D. Wands, JCAP **1606**, 014 (2016) [arXiv:1603.06814].
[2] E. Di Dio, R. Durrer, G. Marozzi and F. Montanari, JCAP **1601**, 016 (2016) [arXiv:1510.04202].
[3] S. Jolicoeur, O. Umeh, R. Maartens and C. Clarkson, in preparation (2016).
[4] D. Bertacca, R. Maartens and C. Clarkson, JCAP **1409**, 037 (2014) [arXiv:1405.4403].
[5] D. Bertacca, R. Maartens and C. Clarkson, JCAP **1411**, 013 (2014) [arXiv:1406.0319].
[6] J. Yoo and M. Zaldarriaga, Phys. Rev. D **90**, 023513 (2014) [arXiv:1406.4140].
[7] E. Di Dio, R. Durrer, G. Marozzi and F. Montanari, JCAP **1412**, 017 (2014) [Erratum: JCAP **1506**, E01 (2015)] [arXiv:1407.0376].
[8] D. Bertacca, Class. Quant. Grav. **32**, 195011 (2015) [arXiv:1409.2024].
[9] A. Kehagias, A. M. Dizgah, J. Noreña, H. Perrier and A. Riotto, JCAP **1508**, 018 (2015) [arXiv:1503.04467].
[10] T. Baldauf, U. Seljak and L. Senatore, JCAP **1104**, 006 (2011) [arXiv:1011.1513].

[11] D. Jeong, F. Schmidt and C. M. Hirata, Phys. Rev. D **85**, 023504 (2012) [arXiv:1107.5427].
[12] A. Challinor and A. Lewis, Phys. Rev. D **84**, 043516 (2011) [arXiv:1105.5292].
[13] S. G. Biern, J. O. Gong and D. Jeong, Phys. Rev. D **89**, 103523 (2014) [arXiv:1403.0438].
[14] E. Villa and C. Rampf, JCAP **1601**, 030 (2016) [arXiv:1505.04782 [gr-qc]].
[15] J. c. Hwang, D. Jeong and H. Noh, Mon. Not. Roy. Astron. Soc. **459**, 1124 (2016) [arXiv:1509.07534].
[16] R. Scoccimarro, S. Colombi, J. N. Fry, J. A. Frieman, E. Hivon and A. Melott, Astrophys. J. **496**, 586 (1998) [astro-ph/9704075].
[17] L. Verde, A. F. Heavens, S. Matarrese and L. Moscardini, Mon. Not. Roy. Astron. Soc. **300**, 747 (1998) [astro-ph/9806028].
[18] R. Maartens, K. Koyama, D. Wands, O. Umeh, C. Clarkson and S. Jolicoeur, in preparation (2016).
[19] P. A. R. Ade *et al.* [Planck Collaboration], Astron. Astrophys. **594**, A13 (2016) [arXiv:1502.01589].
[20] D. Alonso and P. G. Ferreira, Phys. Rev. D **92**, 063525 (2015) [arXiv:1507.03550].
[21] J. Fonseca, S. Camera, M. Santos and R. Maartens, Astrophys. J. **812**, L22 (2015) [arXiv:1507.04605].
[22] M. Bruni, R. Crittenden, K. Koyama, R. Maartens, C. Pitrou and D. Wands, Phys. Rev. D **85**, 041301 (2012) [arXiv:1106.3999].
[23] S. Camera, R. Maartens and M. G. Santos, Mon. Not. Roy. Astron. Soc. **451**, L80 (2015) [arXiv:1412.4781].

Appendix: Redshift evolution of the GR correction kernel

The $\Gamma_I(z)$ functions appearing in the GR correction kernel (12) are given by [3]:[2]

$$\frac{\Gamma_1}{\mathcal{H}^4} = \frac{9}{4}\Omega_m^2\left[6f-5-2\frac{f'}{\mathcal{H}}+\frac{2}{\chi\mathcal{H}}\left(4f-4+\frac{1}{\chi\mathcal{H}}+3\frac{\mathcal{H}'}{\mathcal{H}^2}\right)+4(f-2)\frac{\mathcal{H}'}{\mathcal{H}^2}+3\frac{\mathcal{H}'^2}{\mathcal{H}^4}-\frac{\mathcal{H}''}{\mathcal{H}^3}\right]$$
$$+\frac{9}{2}\Omega_m f\left(11-2f-\frac{4}{\chi\mathcal{H}}-\frac{\mathcal{H}'}{\mathcal{H}^2}\right)+3f^2\left(4-\frac{\mathcal{H}'}{\mathcal{H}^2}\right)$$
$$\frac{\Gamma_2}{\mathcal{H}^3} = \frac{3}{2}\Omega_m f\left[(f-1)(2-f)-\frac{f'}{\mathcal{H}}+\frac{2}{\chi\mathcal{H}}\left(2f+\frac{1}{\chi\mathcal{H}}+3\frac{\mathcal{H}'}{\mathcal{H}^2}\right)+(2f-3)\frac{\mathcal{H}'}{\mathcal{H}^2}+3\frac{\mathcal{H}'^2}{\mathcal{H}^4}-\frac{\mathcal{H}''}{\mathcal{H}^3}\right]$$
$$-\frac{9}{4}\Omega_m^2-3f\left(1+\frac{2}{\chi\mathcal{H}}\right)$$
$$\frac{\Gamma_3}{\mathcal{H}^2} = \frac{3}{2}\Omega_m\left(1-2f+\frac{2}{\chi\mathcal{H}}-3\frac{\mathcal{H}'}{\mathcal{H}^2}\right)-\frac{3\Omega_m'}{2\mathcal{H}}$$
$$\frac{\Gamma_4}{\mathcal{H}^2} = 3f$$
$$\frac{\Gamma_5}{\mathcal{H}^2} = 3\Omega_m f(2-f)+f^2\left[4-\frac{2}{\chi\mathcal{H}}\left(4+\frac{1}{\chi\mathcal{H}}+3\frac{\mathcal{H}'}{\mathcal{H}^2}\right)-3\frac{\mathcal{H}'}{\mathcal{H}^2}-3\frac{\mathcal{H}'^2}{\mathcal{H}^4}+\frac{\mathcal{H}''}{\mathcal{H}^3}\right]$$
$$\frac{\Gamma_6}{\mathcal{H}^2} = f^2\left(1+\frac{\mathcal{H}'}{\mathcal{H}^2}\right)+3\Omega_m f$$
$$\frac{\Gamma_7}{\mathcal{H}^2} = \frac{3}{2}\Omega_m\left[b_1\left(2-\frac{2}{\chi\mathcal{H}}-\frac{\mathcal{H}'}{\mathcal{H}^2}\right)+\frac{b_1'}{\mathcal{H}}\right]+f^2\left[b_1(3-f)-\frac{b_1'}{\mathcal{H}}\right]$$
$$\frac{\Gamma_8}{\mathcal{H}^2} = \frac{9}{4}\Omega_m^2+\frac{3}{2}\Omega_m f\left(3-2f-\frac{4}{\chi\mathcal{H}}-\frac{\mathcal{H}'}{\mathcal{H}^2}\right)+3f^2$$
$$\frac{\Gamma_9}{\mathcal{H}} = -\frac{3}{2}\Omega_m b_1$$
$$\frac{\Gamma_{10}}{\mathcal{H}} = f^2$$
$$\frac{\Gamma_{11}}{\mathcal{H}} = f\left[b_1\left(f-\frac{2}{\chi\mathcal{H}}-\frac{\mathcal{H}'}{\mathcal{H}^2}\right)+\frac{b_1'}{\mathcal{H}}\right]-f^2$$
$$\frac{\Gamma_{12}}{\mathcal{H}} = \frac{3}{2}\Omega_m f$$
$$\frac{\Gamma_{13}}{\mathcal{H}} = \frac{3}{2}\Omega_m f-f^2\left(3+\frac{4}{\chi\mathcal{H}}+\frac{3\mathcal{H}'}{\mathcal{H}^2}\right)$$
$$\frac{\Gamma_{14}}{\mathcal{H}} = -f\left(\frac{2}{\chi\mathcal{H}}+\frac{\mathcal{H}'}{\mathcal{H}^2}\right)$$

[2] Γ_2 in arXiv v2 has been absorbed into Γ_1; the previous $\Gamma_I, I=3,\cdots,14$ have been re-labelled $I=2,\cdots,13$, and the new Γ_{14} term here is a correction to arXiv v2.